Journal of Naval Architecture and Marine Engineering
June, 2014
http://dx.doi.org/10.3329/jname.v11i1.15619 *http://www.banglajol.info*

PROSPECTS OF VIRTUAL OR COMPUTATIONALTOWING TANK FACILITY FOR THE SHIPBUILDING INDUSTRY OFBANGLADESH

M. M. Rahaman[1*], H. Akimoto[2], H. Orihara[3], N.M.G. Zakaria[1] and S. Shabnam[1]
[1]Department of Naval Architecture & Marine Engineering, Bangladesh University of Engineering & Technology, Dhaka-1000, Bangladesh, *Email: mashiurrahaman@name.buet.ac.bd
[2]Visiting Professor, Division of Ocean Systems Engineering (OSE), Korean Advanced Institute of Science & Technology (KAIST), Daejeon 304-701, Republic of Korea
[3]Technical Research Center, Universal Shipbuilding Corporation, 1-3 Kumozu-Kokan-cho, Tsu 514-0398, Japan

Abstract:

Shipbuilding is on the verge of blooming into the major foreign revenue-earning industry in Bangladesh. A number of export-oriented shipyards are developed to build different kinds of ships for local and international clients. For designing a ship, model testing facilities are required not only to predict power requirements but also to evaluate its performance in actual sea operation. At present, Bangladesh does not have this facility. Also carrying out model testing is very expensive and time consuming. Therefore, now-a-days a number of the shipyards in the world are using virtual or computational towing tank facility. Due to improvement of solution algorithm for handling non-linear problem and computational infrastructure, computational or virtual towing tank can be used as a replacement of physical towing tank. In the present study, a numerical or computational towing tank technique named WISDAM which is developed at The University of Tokyo, Japan is described with its applicability in the perspective of Bangladesh shipbuilding industries.

***Keywords*:** Computational fluid dynamics, RaNS, virtual towing tank, shipbuilding

1. Introduction

Bangladesh has a strong background in building ships and was one of the leading centers of building inland and ocean-going ships in Asia during the 15th and 17th century. Nature has adored Bangladesh with more than 200 rivers with a total length of about 22,155km plus an extensive coast line of the Bay of Bengal. Due to the long history of maritime activities and also a natural geographical advantage, there are presently more than 100 shipbuilding and ship-repair yards to cater for the international and domestic needs in Bangladesh.

As a primary mode of transport, almost one fourth of the population of Bangladesh uses water transport. The river network of Bangladesh extends to 8,300 km during the rainy season from 5,200 km during dry season. Water transport is the cheapest mode of transport and therefore, it has become one of the most important modes of transport for developing countries like Bangladesh. Various types of inland and coastal ships constructed during 2005-2009 are described in Table 1. Almost 95% of the vessels mentioned in Table 1 are designed by local design farms without conducting any physical or numerical experiments. Therefore, these vessels encounter accidents regularly and causing loss of valuable lives and resources.

Table 1: Inland ship constructed during 2005-2009*(Source: Hossain, 2010)*

Sl. No.	Types of vessels	Capacity	2005	2006	2007	2008	2009
1	Oil tanker	500-2000	12	8	1	0	1
2	Cargo vessel	1500-3000	60	95	30	20	50
3	Passenger vessel	200-1200 pax	12	8	3	1	2
4	Small dredger	2-10	35	25	18	12	13
5	Sand carrier	200-400	150	160	40	30	100
6	Barge	200-800	15	14	3	3	10
7	Tug boat	20-200	2	1	0	0	0
8	Dumb dredger	200-800	15	10	2	1	3
9	Self propelled barge	100-500	6	7	2	1	1
10	Small launch	Below 200 pax	10	22	8	9	20

 Received on: July 2013

Since William Froude (ca. 1850) ship design is based on towing tank tests, which have been standardized beginning in 1933 by procedures developed under the auspices of the International Towing Tank Conference (ITTC) at its tri-annual meetings. The advent of computer technology and computational fluid dynamics (CFD) methods offers an alternative to the traditional build and test design approach, i.e., simulation based design (SBD). It has been conjectured that SBD will offer innovative approaches to design and out-of-the box concepts with improved performance.

CFD for ship hydrodynamics is well developed with advanced capabilities for resistance and propulsion, sea-keeping, and maneuvering as evidenced by the ship hydrodynamics CFD workshops and bi-annual Office of Naval Research (ONR) Symposiums on Naval Hydrodynamics (SNH). One of the leading ship hydrodynamics CFD codes and of present interest is WISDAM, which has been developed at The University of Tokyo, Japan. The capabilities of ship hydrodynamics CFD codes have largely been demonstrated mimicking typical towing tank tests using the experimental data for validation of the simulations, including both global and local flow variables (Longo et.al. 2007). Once validated, CFD thus far has largely been used for design analysis, but with its current interdisciplinary capability including global optimization methods(Campana et. al., 2006) and emerging multidisciplinary capability it assures in short time the reality of SBD. Recently, CFD has shown its usefulness inconceptual design for high-speed sealift concepts (Stern et. al., 2006). Herein, the concept of a computational towing tank is implemented to show that CFD and SBD have a potential to aid the design process. The idea of a numerical towing tank is not new, as the name has been used for an annual European workshop, most recently Numerical Towing Tank Symposium (NUTTS); however, herein we demonstrate different possibilities and the full potential of the concept. It will be shown that both resistance and propulsion tests can be conducted in a unique and efficient manner not possible or highly difficult using a physical towing tank.

2. Challenges in Maritime Design

Hydrodynamic performance of ships is one of the most decisive factors for quality, economy and safety in waterborne transportation. Analysis and optimization of the hydrodynamic performance or behavior of ships at sea is a lengthy, time consuming process, sparsely supported by modern computational techniques. This element which is prominent in the design process for ships and maritime structures is a limiting factor for the overall performance of the maritime industry. Improving this situation will clearly uplift the performance of shipbuilding and overall maritime industry. Being able to fix design constraints for a typical one-of-a-kind product early in the design process allows for a substantially improved accuracy in the production planning and cost evaluation processes. Improving global design and optimization processes will thus have direct as well as indirect-via a shortened production lead time-influences on the products and production costs.

3. Present Status of Maritime CFD

Numerical treatment of fluid flow for maritime crafts are much more complex than other types of vehicle because of special environmental treatments associated with its operation for example sailing at a free surface. Academic and research organizations have devoted long potential on numerical simulations in the maritime field accompanying traditional model testing.

Numerical or computational fluid dynamics (CFD) methods have been developed mostly with a dedicated field of application in mind. Examples are potential theory based strip methods, wave resistance or propeller codes. Concentration on particular applications has caused a large variety of methods, based on different methods and technologies to be developed in the past. Today's developments are without any doubt helpful tools to analyze hydrodynamic behavior, but it must be clearly noted that they hardly allow for integrated analysis of a variety of different objectives. This will still call for sequential process applying a variety of different methods and suffer from often complex data exchange and conversion process.

Experimental or model tank testing has a long tradition and, due to its history and experience gained with calibration results, a wide acceptance in terms of accuracy of predicted results. Today experimental results are still the measure with which to compare all numerical results. Although there have been significant improvements in the quality or accuracy of CFD predictions over time, it may be noted here that there is still a lack of accuracy associated with many numerical flow predictions methods.

4. WISDAM Technique

Unsteady Reynolds averaged Navier-Stokes based WISDAM codes developed by Orihara et.al. (2000, 2002, 2003 and 2004) for predicting hydrodynamic characteristics of practical ship hull form with the capability of

handling 6 (six) DOF motions. At present, WISDAM codes are used by IHI Corporation, Japan and other renowned shipyards and shipbuilding industry in Japan and Republic of Korea.

4.1 Co-ordinate system

WISDAM method uses three different sets of orthogonal co-ordinate systems, space-fixed o-xyz, body-fixed O-*XYZ* and translation co-ordinate system O-$X_0Y_0Z_0$ shown in Fig.1. These co-ordinate systems relates in the following manner.

$$(X_0, Y_0, Z_0)^T = (x, y, z)^T - r_c(t) \tag{1}$$

$$(X, Y, Z)^T = E(\Phi, \Theta, \Psi).(X_0, Y_0, Z_0)^T \tag{2}$$

Here, Euler angles, $\Omega = (\Phi, \Theta, \Psi)$ which is transformation matrix as

$$E(\Phi,\Theta,\Psi) = \begin{bmatrix} \cos\Theta\cos\Psi & \cos\Theta\sin\Psi & -\sin\Theta \\ \sin\Phi\sin\Theta\cos\Psi - \cos\Phi\sin\Psi & \sin\Phi\sin\Theta\sin\Psi + \cos\Phi\cos\Psi & \sin\Phi\cos\Theta \\ \cos\Phi\sin\Theta\cos\Psi + \sin\Phi\sin\Psi & \cos\Phi\sin\Theta\sin\Psi - \sin\Phi\cos\Psi & \cos\Phi\cos\Theta \end{bmatrix} \tag{3}$$

and $r_c(t)$ is the position vector of the center of gravity of the ship defined in o-xyz.

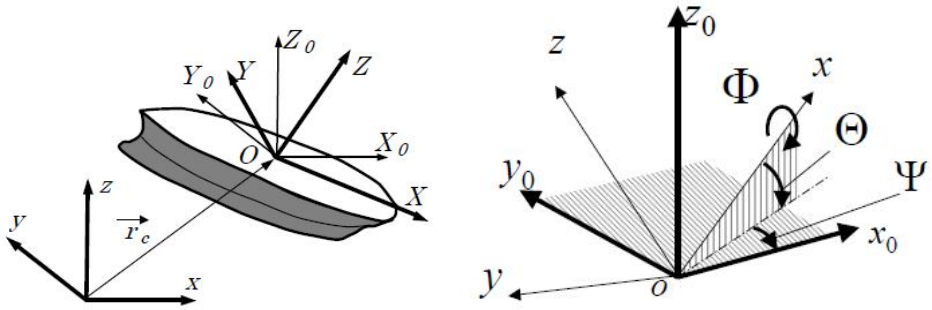

Fig. 1: Definition of co-ordinate systems and Euler angles, Orihara [2003]

4.2 Governing equations

Reynolds averaged Navier-Stokes equation and the continuity equations are solved on the overlapping grid system using finite volume method. In non-inertial co-ordinate system, the RaNS and continuity equations are expressed in the integral form for a control volume Ω as;

$$\int_\Omega \frac{\partial u}{\partial t} dV + \int_\Omega T dS = \int_\Omega K dV \tag{4}$$

$$\int_{\partial\Omega} u.dS = 0 \tag{5}$$

where u is the fluid velocity vector, T is the fluid stress tensor and K is the body force vector accounting for the inertial effect on fluid.

All of the fluid variables are made dimensionless with respect to constant reference velocity U_0, ship length L and the density of fluid. The dimensionless parameters, Reynolds number (R_e) and Froude number (F_n) are defined as

$$R_e = \frac{U_0 L}{\nu} \qquad F_n = \frac{U_0}{\sqrt{gL}} \tag{6}$$

where ν and g are the dynamic viscosity of fluid and the gravitational acceleration respectively.

The fluid stress tensor T is expressed as

$$T = uu + \phi I - \frac{1}{R_e}\left[\nabla u + (\nabla u)^T\right] + u'u' \tag{7}$$

where I is the identity tensor, ∇ is the gradient operator, $(.)^T$ denotes the transport operator, $u'u'$ is the Reynolds stress and ϕ is the non-dimensionalized pressure excluding the hydrostatic component defined as

$$\phi = p + \frac{z}{F_n^2} \tag{8}$$

where z is the vertical up and p is the static pressure of the fluid.

The body force vector K is given as follows

$$K = -2\omega \times u - \omega \times (\omega \times r) - \frac{d\omega}{dt} \times r - \frac{dV}{dt} \tag{9}$$

where ω is the angular velocity vector about body fixed co-ordinate system O-XYZ, r is the position vector defined in O-XYZ, V is the translating velocity of the origin of the body-fixed system. The term in the right-hand side of eq. (9) are the Coriolis force, the centrifugal force, the angular acceleration force and the translating acceleration force respectively.

4.3 Free-surface treatment

Treatment of free-surface is based on density function method. In WISDAM, solving the following transport equation of density function ρ_m satisfies the kinematic condition of free surface.

$$\int_\Omega \frac{\partial \rho_m}{\partial t} dV = -\int_\Omega dS.u\rho_m \tag{10}$$

where u is the velocity vector of fluid, density function ρ_m defined in the entire computational region as,

$$\rho_m \equiv \begin{cases} 1 & in\ fluid\ region \\ 0 & in\ external\ region \end{cases} \tag{11}$$

Equation (10) is discretized by finite-volume method and solved in a time marching way. The location of free surface is as the iso-surface of ρ_m =0.5. Extrapolation of pressure and velocity components above the free surface satisfies the free surface dynamic condition.

To evaluate turbulent viscosity in the flow field, blended Baldwin-Lomax zero equation model and Dynamic Sub-Grid Scale (DSGS) model is used. The local turbulent velocity is determined by weighted average of these two models.

4.4 Computational domains and grids

For the implementation of the interaction of incident waves and the resultant ship motions, overlapping grid systems are employed in WISDAM. By employing overlapping grid systems, the total simulation domains (shown in Fig.2) are divided into two as inner solution domain and outer solution domain. The inner solution domain covers the vicinity of the hull surface, where high resolution mesh (C-H type for half hull; O-H type for full hull) is generated to capture the free surface. The outer solution domain is located at a several ship length away from the hull surface. In each solution domain, structured computational mesh is generated independently using PointwiseV16.04R3. To avoid green water loading on deck, the hull surface is extended in upward direction to cover the deck.

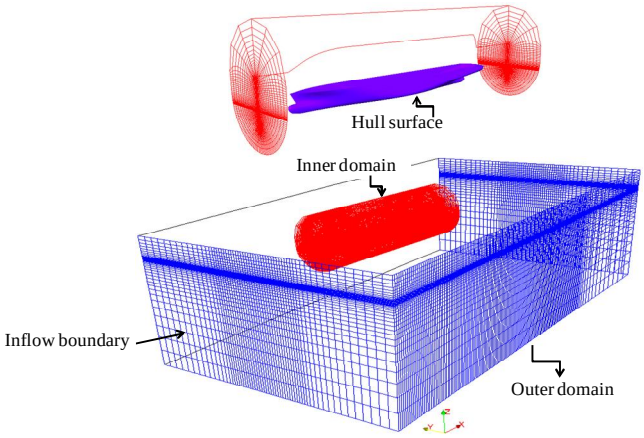

Fig.2: Computational domains of WISDAM

4.5 Flow simulation

The motion of the ship is simultaneously solved by combining the equations of motions of the ship body with the flow computation. Since, non-deforming grid is used, the flow computation in the near filed is performed on the non-inertia co-ordinate system fixed to the body of the ship. The effect of the ship motion on the flow solution is taken into account by adding inertia forces as the body force *K* in the right-hand side of Eq. (4).

4.6 Wave generation

In WISDAM, incident waves are generated based on linear wave theory by which wave velocity potential is derived as

$$\Phi = \varsigma_A c \frac{\cosh \kappa(d+z)}{\sinh(\kappa d)} \sin\{\kappa(-x\cos\chi - y\sin\chi) - \omega t\} \tag{12}$$

Further, if we assume that water depth tends to infinity, then the flow velocity u and arbitrary quantity ϕ in the space-fixed co-ordinate system can be described as,

$$u = \begin{pmatrix} u_w \\ v_w \\ w_w \end{pmatrix} = \begin{pmatrix} -\cos\chi\varsigma_A\omega e^{\kappa z}\cos\{\kappa(-x\cos\chi - y\sin\chi) - \omega t\} \\ -\sin\chi\varsigma_A\omega e^{\kappa z}\cos\{\kappa(-x\cos\chi - y\sin\chi) - \omega t\} \\ \varsigma_A\omega e^{\kappa z}\sin\{\kappa(-x\cos\chi - y\sin\chi) - \omega t\} \end{pmatrix} \tag{13}$$

$$\phi_w = \varsigma_A\omega c e^{\kappa z}\sin\left\{\kappa(-x\cos\chi - y\sin\chi) - \omega t\right\} - \frac{\omega^2\varsigma_A^2}{2}e^{2\kappa z} \tag{14}$$

Here,

$u_w = \frac{\partial\Omega}{\partial x}, v_w = \frac{\partial\Omega}{\partial y}, w_w = \frac{\partial\Omega}{\partial z}$

ϕ_w = static pressure of incident waves.

Incident waves are generated on outer solution domain. When waves enter into inner solution domain, boundary conditions with the interaction of (u_w, v_w, w_w) and uniform velocity $(U_0, 0, 0)$ transform the formula into the following.

$$u = \begin{pmatrix} u \\ v \\ w \end{pmatrix} = \begin{pmatrix} U_0 - \cos\chi\varsigma_A\omega e^{\kappa z}\cos\{\kappa(-x\cos\chi - y\sin\chi) - \omega t\} \\ -\sin\chi\varsigma_A\omega e^{\kappa z}\cos\{\kappa(-x\cos\chi - y\sin\chi) - \omega t\} \\ \varsigma_A\omega e^{\kappa z}\sin\{\kappa(-x\cos\chi - y\sin\chi) - \omega t\} \end{pmatrix} \quad (15)$$

Moreover, the relationship between space-fixed co-ordinate, o-xyz and translation co-ordinate O-$X_0Y_0Z_0$ is expressed as

$$\begin{pmatrix} x \\ y \\ z \end{pmatrix} = \begin{pmatrix} X_0 - U_0 t + \dfrac{U_0 T_{acc}}{2} \\ Y_0 \\ Z_0 \end{pmatrix} \quad (16)$$

5. Application of WISDAM Technique

Computational results of WISDAM were already validated with towing tank experimental results for different types of ships at various Froude's number with various conditions of wave length-ship length ratio, λ/L and wave amplitude-ship length ratios, ζ/L in regular and irregular head and oblique waves. All calculations were performed with 2 (two) degrees of freedom i.e. heave and pitch free conditions. In this section, some of the results are presented to show the capability of WISDAM and its applicability to use in initial ship design process.

5.1 Ship model

Numerical or computational results of container ship models named SR108, KCS; tanker ship model SR221C; bow-series model M58F0, M58F1 are presented.

5.1.1 Container ship model

Ship model SR108 was designed by National Maritime Research Institute (NMRI), Japan and KCS is developed by Korean Ocean Research and Development Institute (KORDI).Figs. 3(a) and 3(b) show the body plan of SR108 and KCS respectively.

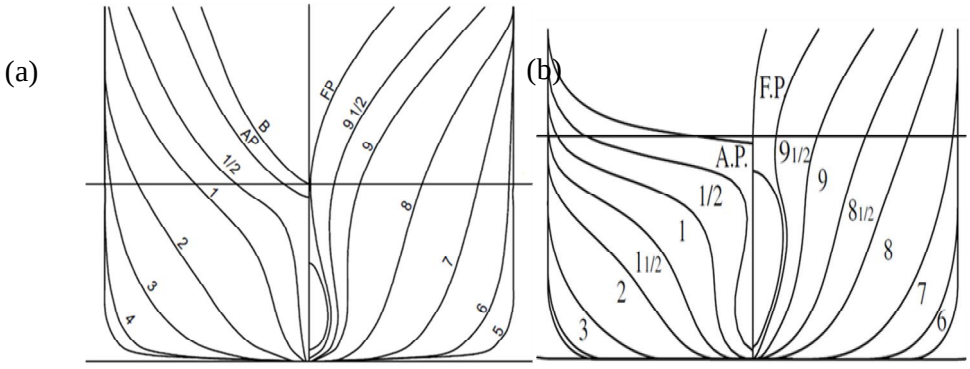

Fig. 3: Body plan of (a) SR108 and (b) KCS

5.1.2 Tanker ship model

Fig. 4 shows locations of pressure point pick-up for validation of local pressure on the body plan of a tanker ship model, SR221C.

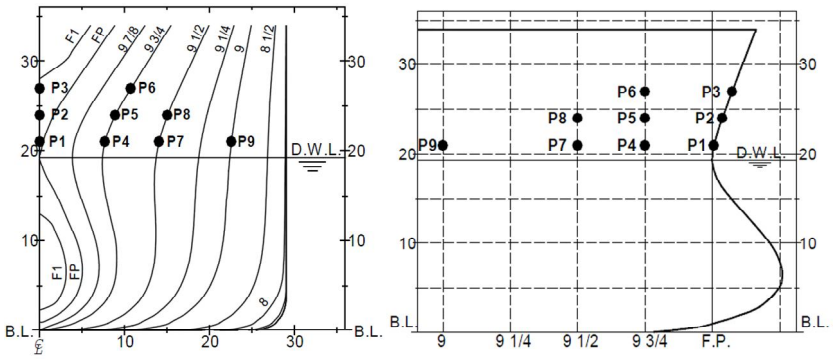

Fig.4: Locations of pressure pick-ups on tanker ship model SR221C, Orihara [2004]

5.1.3 Bow-series model

The M58 series consists of two models with different bow shapes, different in the hull portion above the design water line (DWL). The bow shape of M58F1 differs from that of the original form (M58F0) in both the bow profile and body plan ahead of S.S. and 9 ½ as shown in Fig. 5. M58F1 has an extremely long-protruding bow shape which is expected to reduce added resistance in waves by reducing the entrance angle of the waterline above DWL.

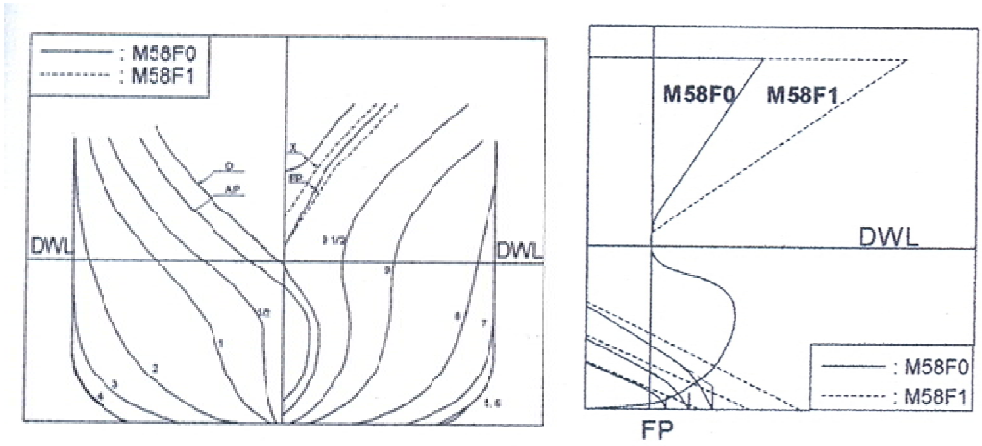

Fig.5: Body plans and bow profiles of M58 series models, Orihara [2003]

5.2 Ship motions in regular head wave

Fig. 6 shows the comparison of Response Amplitude Operator (RAO) of heave and pitch motion of SR108 at Froude No., F_n=0.25 and ζ/L= 0.01 in head wave. The amplitude of heave and pitch motions are made dimensionless with respect to wave amplitude and wave slope respectively. The amplitudes of the ship's motions are obtained by harmonic analysis of computed time histories of ship's motion, where the first harmonic is taken as the motion amplitude. Fig. 7 shows the comparison of time history of heave and pitch motion for KCS at F_n=0.33, λ/L=1.33 and ζ/L= 0.0112 in head wave. Figs.8 and 9 show the comparison of RAO's of heave and pitch motion for M58 model series at F_n=0.224 and for SR221C model series F_n=0.15 in head wave respectively. It is seen from Figs.6 ~ 9 that WISDAM predicted ship motions accurately with towing tank experiments for all the cases. The possible reason for accurate predictions of ship motions is the exact treatment of the hull surfaces and the free surface boundary conditions in WISDAM. Since ship's motion has a noticeable effect on the surface pressures, this copes with the good agreement of calculated surface pressures with experimental data.

Since the uncertainty of the experimental data is not evaluated, in general, it may be said that it is 1% of the amplitude of the incident wave for the amplitude of heave motions and within 1% of the mean slope of the incident wave for the amplitude of pitch motions.

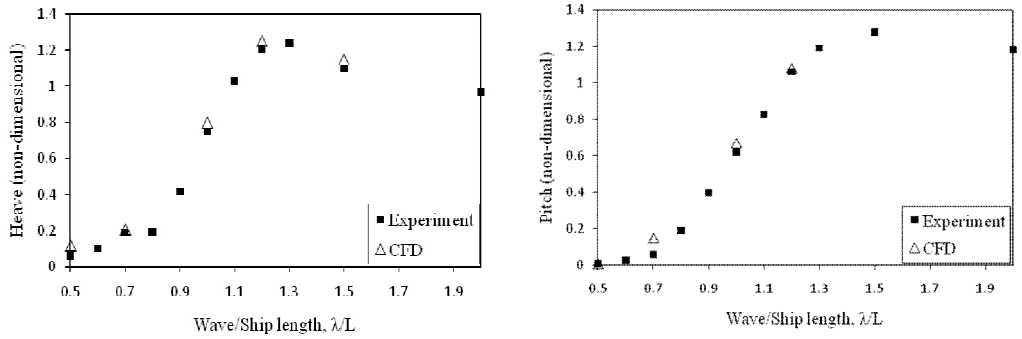

Fig.6: Response amplitude operator of heave and pitch motion of SR108 at F_n=0.25 and ζ/L= 0.01 in head wave

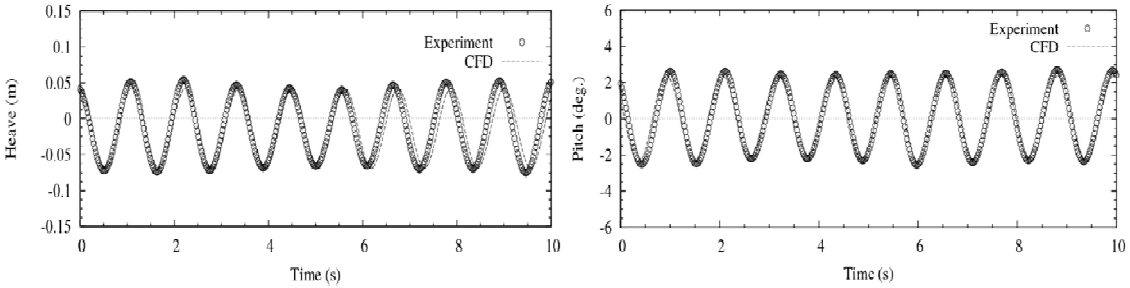

Fig.7: Comparison of time history of heave and pitch motion for KCS at F_n=0.33, λ/L=1.33 and ζ/L= 0.0112 in head wave

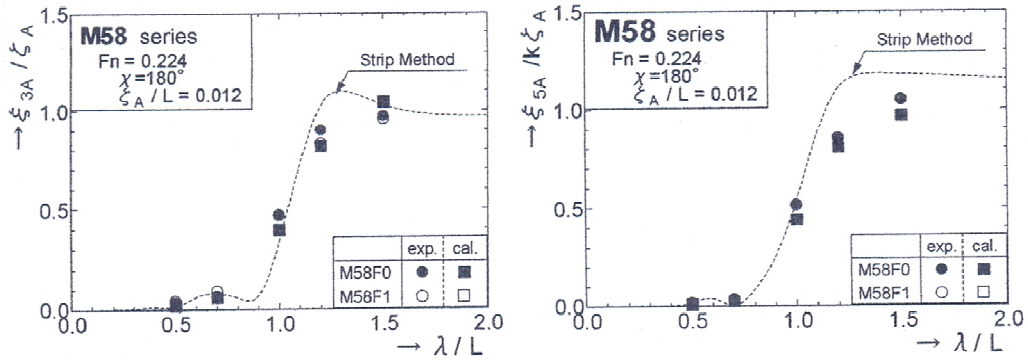

Fig.8: Comparison of RAO's of heave and pitch motion for M58 model series at F_n=0.224 in head wave,Orihara [2003]

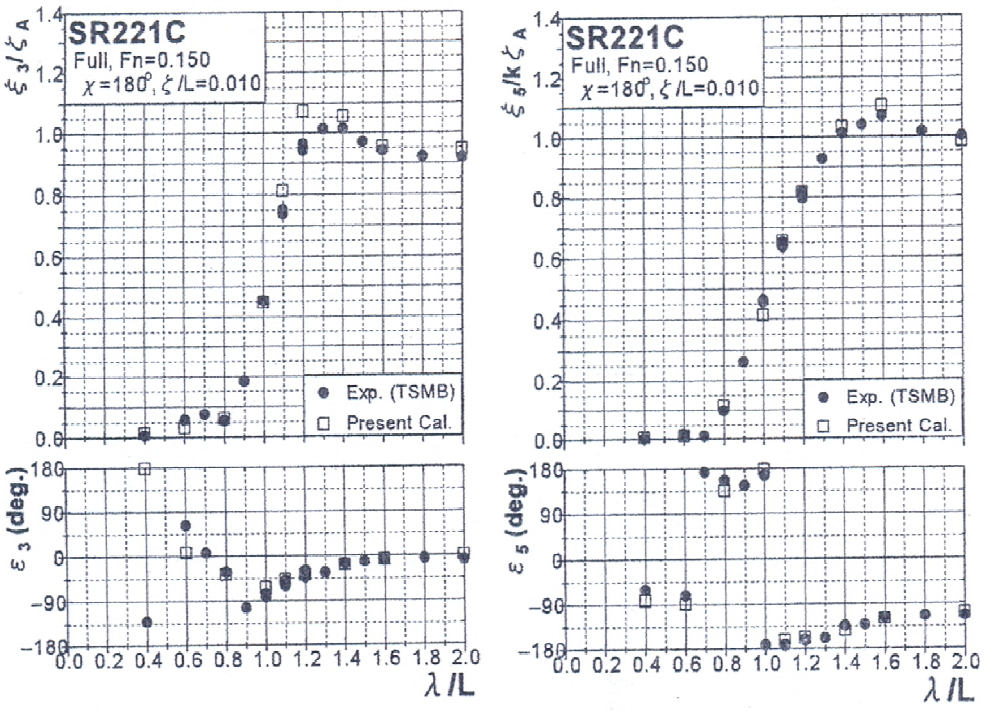

Fig.9: Comparison of RAO's of heave and pitch motion for SR221C at F_n=0.15 in head wave

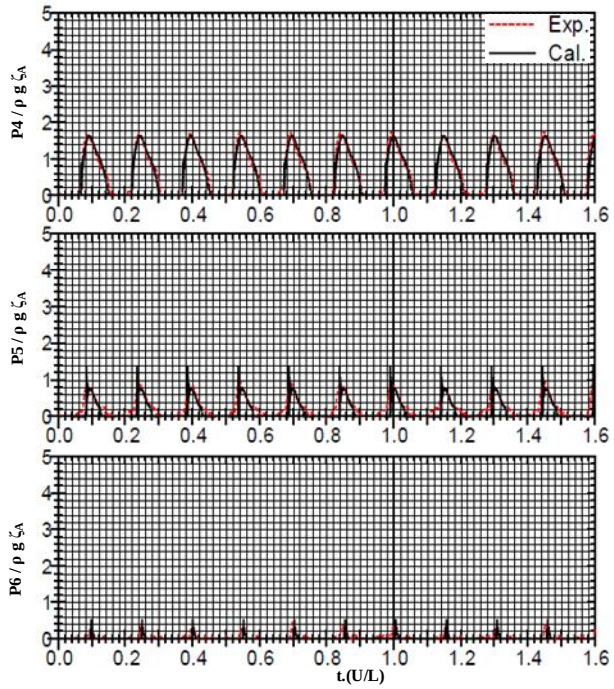

Fig.10: Comparison of time history of surface pressures on tanker ship model SR221C in regular head waves at Fn=0.150, λ/L=0.4 and ζ_A/L=0.01, Orihara [2004]

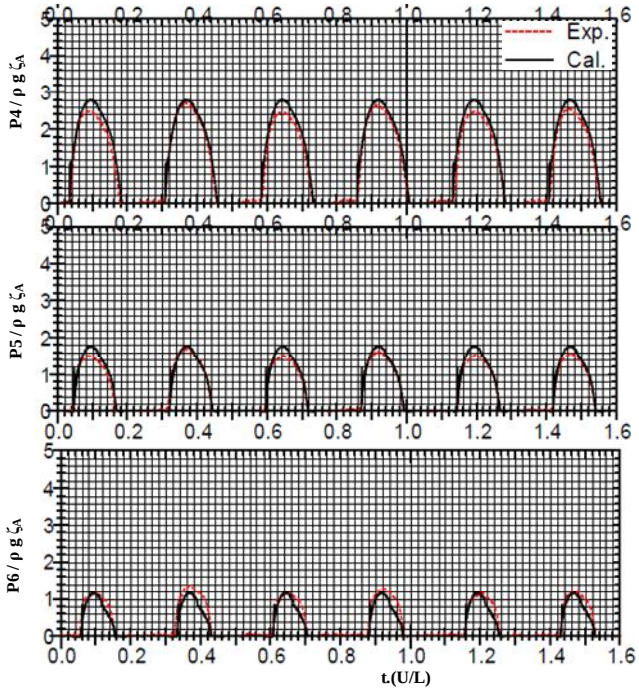

Fig.11: Comparison of time history of surface pressures on tanker ship model SR221C in regular head waves at Fn=0.150, λ/L=1.00 and ζ_A/L=0.01, Orihara [2004]

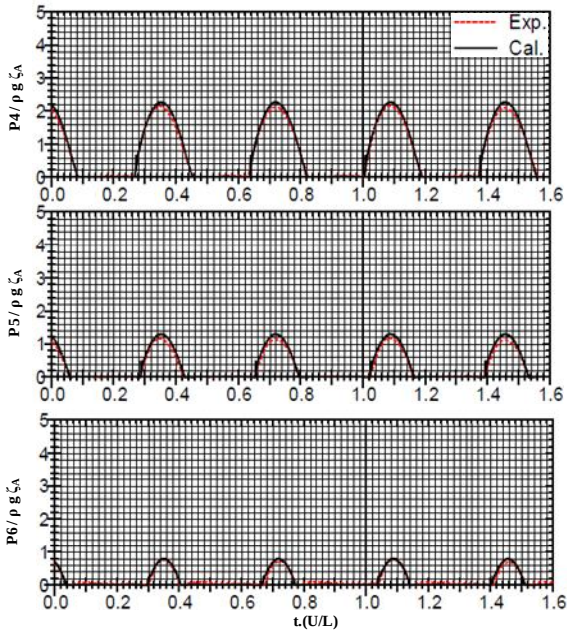

Fig.12: Comparison of time history of surface pressures on tanker ship model SR221C in regular head waves at Fn=0.150, λ/L=1.6 and ζ_A/L=0.01, Orihara [2004]

Time history of local pressure is evaluated at six points on the flare region of tanker model SR221C, shown in Fig. 4. Locations of points are chosen based on the high pressure region on the bow flare. Local pressure is non-dimensionalized based on density of water, ρ, gravitational acceleration, g and local wave amplitude.

Comparison of time histories of hull surface pressures are shown in Figs.10~12 for the cases λ/L= 0.4, 1.0 and 1.6 at Fn=0.150 and ζ_A/L=0.01. In present study, the pressures are defined as the difference relative to the atmospheric pressures. So, the pressure is zero when the pressure gauges exposed in the air. Since the gauges are place above the still water level, all the gauges experienced the exposure in the air for all the cases of wave lengths. As can be seen in Figs. 10 ~12, calculated results are in good agreement with the experimental data. The calculated histories capture time histories from triangular shape to rounded one with the increase in the length of incident waves.

5.3 Ship motions in regular oblique wave

Figs. 13(a) ~ 13(b) show the comparison of Response Amplitude Operator (RAO) of heave and pitch motion for SR108 at F_n=0.25 and ζ/L= 0.01 in 120 deg. oblique wave. Present numerical method, WISDAM predicted peak value of heave and pitch motions well with experiments.

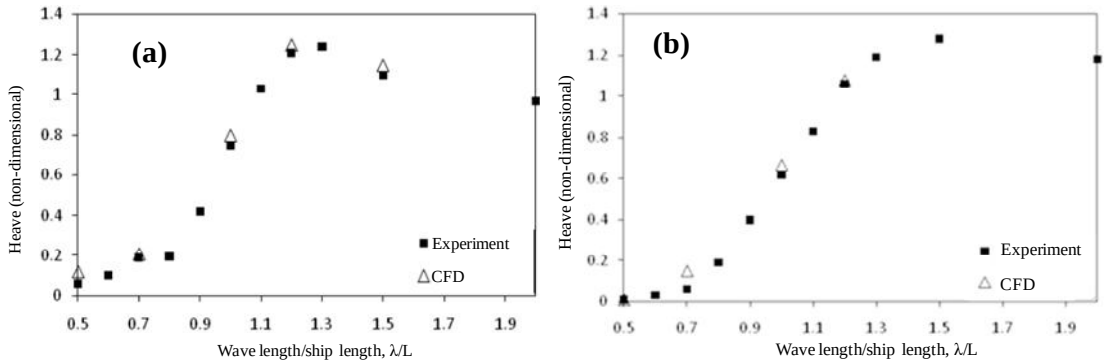

Fig.13: Response amplitude operator for SR108 at F_n=0.25 and ζ/L= 0.01 in 120 deg. oblique wave; (a) heave motion and (b) pitch motion

5.4 Added resistance in regular head wave

Fig. 14 shows the comparison of Response Amplitude Operator (RAO)'s of added resistance for SR108 at F_n=0.250, 0.275and 0.300 in waves of ζ/L= 0.01. Although, some discrepancies can be seen in Fig. 14, the computed results agree well with experimental results in all the cases.

Fig. 15 shows the comparison of time history of total drag for ship model KCS at F_n=0.26, λ/L=2.00 and ζ/L= 0.0167. It is seen from Fig. 15 that WISDAM under predicted the total drag for case of KCS. The possible reasons for this discrepancy in total resistance are due to the way of ship model towed during experiment. In the experiment, the model is mounted in two posts. Therefore, the system is not completely stiff. The ship may surge when it moves through waves. So, during experiment the action is like the model is towed in a spring. However, in numerical method, the model is towed in an ideal stiff setup. It means the possibility of surging during numerical simulation is zero. The result could be that the shape of the time series for the resistance obtained with different systems could be different and that the signals, therefore cannot be directly compared at a given time instance.

(Simonsen et. al. , 2008) compared their numerical method (RaNS based CFD code CFDSHIP-IOWA) with the same experimental results of present analysis and a strong disagreement was observed for resistance data. They concluded that the data may be deficient.

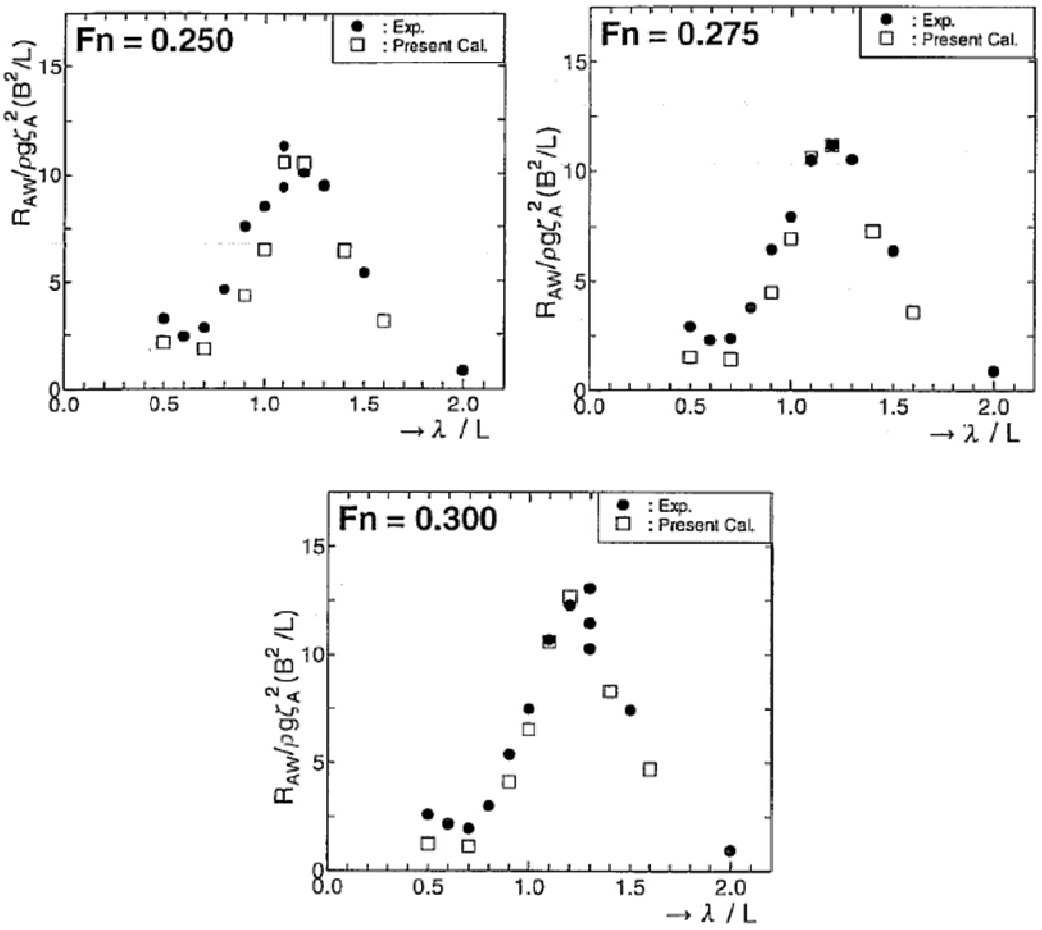

Fig.14: Comparison of RAO's of added resistance for SR108 at F_n=0.250, 0.275and 0.300 in waves of ζ/L= 0.01

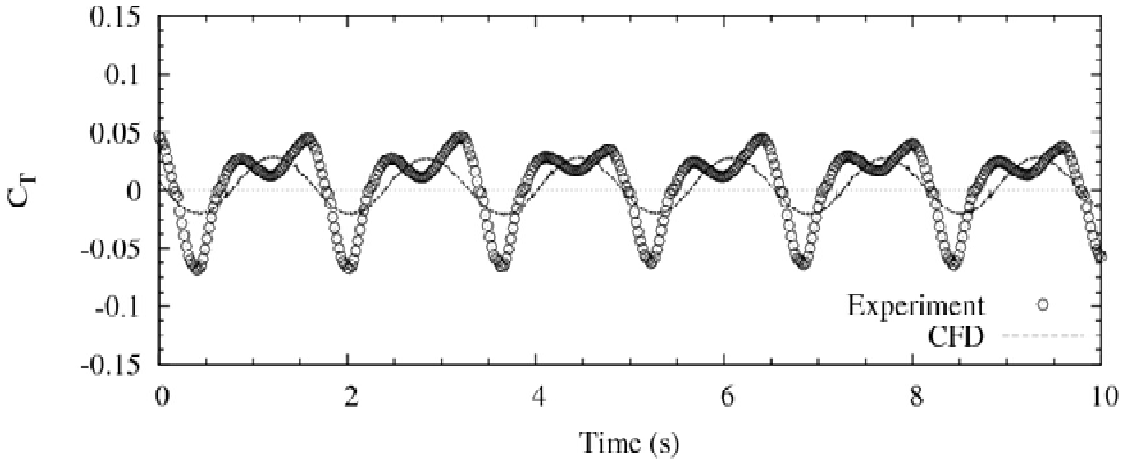

Fig.15: Comparison of time history of total drag coefficient, C_T for KCS at F_n=0.26, λ/L=2.00 and ζ/L= 0.0167 in head wave

Comparison of RAO's of added resistance for SR221C at F_n=0.26 in head wave is shown in Fig.16. Though the predicted results slightly overestimate the experimental data, the calculated results agree well with the experimental results.

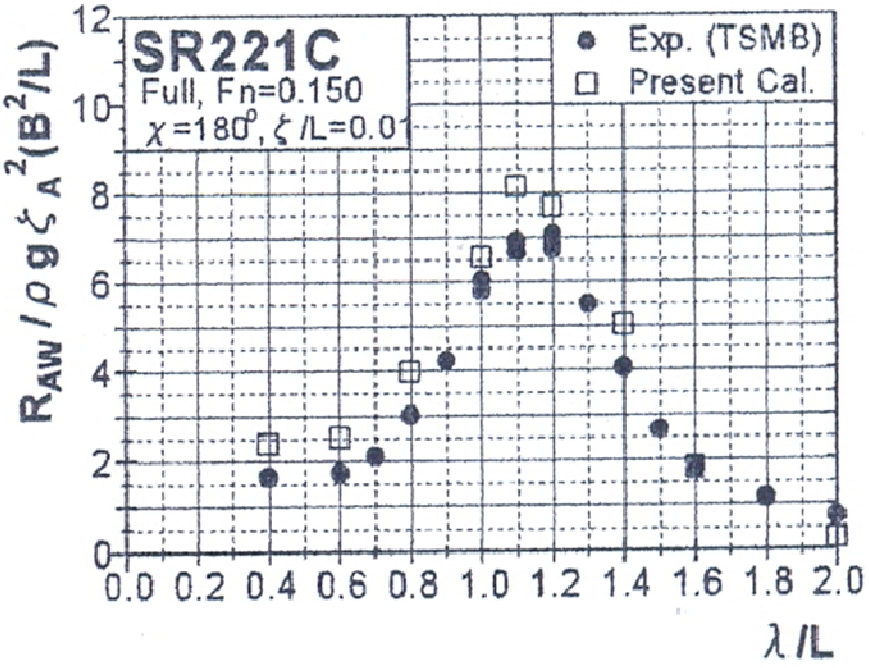

Fig.16: Comparison of RAO's of added resistance for SR221C at F_n=0.26 in head wave

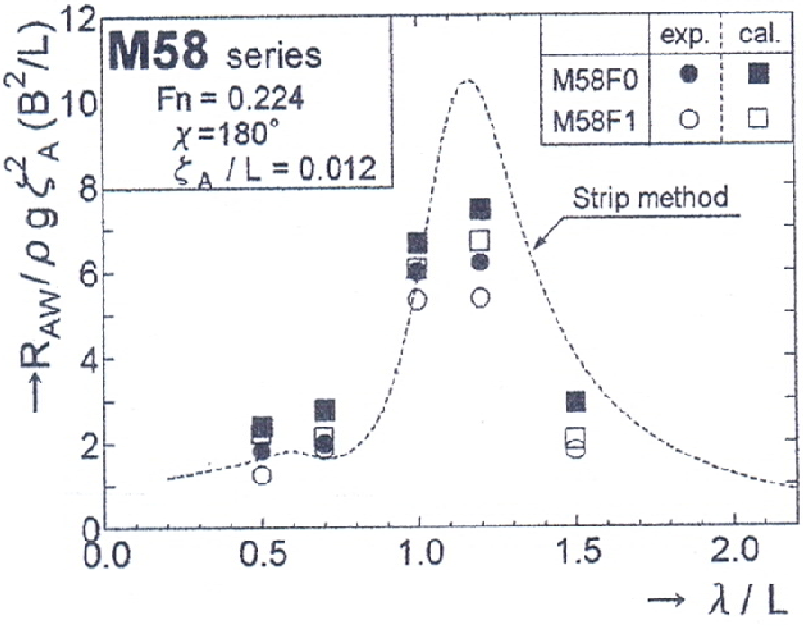

Fig.17: Comparison of RAO's of added resistance for M58 model series at F_n=0.224 in head wave, Orihara [2004]

Fig. 17 shows the comparison of added resistance for M58 model series at F_n=0.224 in head wave. Although, some calculations slightly over predicts the experiment, the relative magnitude of added resistance between the models i.e. the reduction in added resistance due to the bow shape modifications is well predicted. For all the wave length cases, the computed added resistance for M58F1 is smaller than for M58F0 by nearly the same amount as measured difference in added resistance in the experiment.

Conclusion

A RaNS based virtual or computational towing tank technique WISDAM is described. The accuracy of the predictions is validated by comparing time histories and Response Amplitude Operator (RAO)of surface pressures, ship motions and added resistance. Two container ship models named SR108 and KCS, tanker ship model SR221C and bow-series models M58F0 and M58F1 are chosen for assessment. It is seen that WISDAM can predict the ship motions and added resistance well with experiments for these ships. Although the degree of accuracy of predictions is not fully satisfactory but the present CFD results show a superior availability than other existing analytical methods.

Also, since at present physical experimental facilities for maritime industry like towing tank are not available in Bangladesh, WISDAM can be a better alternative tool for the assessment of ship performance in waves and the development of hull forms with superior performance in waves.

Acknowledgement

This research was supported by WCU (World Class University) program through the National Research Foundation of Korea funded by the Ministry of Education, Science and Technology (R31-2008-000-10045-0).

References

Campana, E. F., Peri, D., Tahara, Y., and Stern, F. (2006): Shape optimization in ship hydrodynamics using computational fluid dynamics, Computational Methods Appl. Mech. Eng., 196(1–3), pp. 634–651. http://dx.doi.org/10.1016/j.cma.2006.06.003

Hossain, K.A.(2010): Evaluation of potential, prospects and challenge of Bangladesh shipbuilding in the light of global context, M.Sc. Engg. Thesis, Department of Naval Architecture & Marine Engineering, Bangladesh University of Engineering & Technology (BUET), Dhaka-1000, Bangladesh

Longo, J., Shao, J., Irvine, M., and Stern, F. (2007): Phase-averaged PIV for the nominal wake of a surface ship in regular head waves, ASME J. Fluid Engg., 129(5), pp. 524–540.http://dx.doi.org/10.1115/1.2717618

Orihara, H. and Miyata, H. (2000): Numerical simulation method for flows about a semi-planing boat with a transom stern, Journal of Ship Research, vol. 44, No.3, pp.170-185.

Orihara, H. (2002): Validation of numerical method for predicting hydrodynamic characteristics of a high-speed ship, 24th Symposium on Naval Hydrodynamics, Fukuoka, Japan.

Orihara, H. and Miyata, H. (2003): Evaluation of added resistance in regular incident waves by computational fluid dynamics motion simulation using an overlapping grid system, Journal of Marine Science and Technology, vol. 6, pp. 47-60.http://dx.doi.org/10.1007/s00773-003-0163-5

Orihara, H. and Miyata, H. (2004): CFD performance simulation method for the prediction of life cycle fuel consumption, 25th Symposium on Naval Hydrodynamics, Newfoundland, Canada.

Simonsen, C., Otsen, J. and Stern, F. (2008): EFD and CFD for KCS heaving and pitching in regular head waves, Proceedings of 27th Symposium on Naval Hydrodynamics, Seoul, Korea, pp. 302-320.

Stern, F., Carrica, P. M., Kandasamy, M., Gorski, J., O'Dea, J., Hughes, M.,Miller, R., Hendrix, D., Kring, D., Milewski, W., Hoffman, R., and Gary, C. (2006): Computational hydrodynamic tools for high-speed cargo transports, The SNAME Transactions, 114, pp. 55–81.